Subsurface Structure, Fault Zone Characteristics, and Stress State in Scientific Drill Holes of Taiwan Chelungpu Fault Drilling Project

by Jih-Hao Hung, Kuo-Fong Ma, Chien-Yin Wang, Shen-Rong Song, Hisao Ito, Weiren Lin, and En-Chao Yeh

doi:10.2204/iodp.sd.s01.27.2007

Introduction

The 1999 Chi-Chi earthquake (M_w7.6) produced a >90-km-long surface rupture zone along the north-south trending, west-vergent Chelungpu fault. The most striking feature of the coseismic displacement field is that areas of large surface displacement lie above the footwall ramp of the thrust and at the northern termination (up to 12 m). An important question that needs to be addressed is what physical properties or dynamic processes within the fault zone cause large coseismic displacements in the northern segment. Hypotheses that have been proposed include 1) change of the fault-plane geometry (Yue et al., 2005); 2) static (long-term) physical properties such as intrinsic low coefficient of friction, high pore-pressure, and solution-transport chemical processes; and 3) dynamic change of physical properties during slip. To address the above questions two holes (A and B) were drilled for the Taiwan Chelungpu Fault Drilling Project (TCDP) during 2004–2005 at Dakeng, west-central Taiwan, where large surface slip (~10 m) was observed. Continuous coring and geophysical downhole logging in two holes 40 meters apart were completed from a depth of 500–2003 m (Hole A) and 950–1350 m (Hole B). Data from the drilled holes provide a unique opportunity to understand deformation mechanisms and physical properties of the Chelungpu fault where large slip occurred in the Chi-Chi earthquake.

Subsurface Structure and Fault-Zone Characteristics

Subsurface structure, stratigraphy, and corresponding log depth encountered in Hole A are shown in Fig. 1. Regional bed attitude above FZA1712, identified from cores and FMI/FMS images in Hole A and from correlation of fault zones between Hole A and Hole B, is trending N15°-E21°, dipping 20°–40° (30° on average) toward SE. Nonetheless, intervals of increasing (from 30° to 75°) or decreasing (from 70° to 20°) dip, as well as changes of dip azimuth, appear across fault zones. A gradual increase of bedding dip with depth starts from FZA1712, and a drastic change of dip from 20°–40° to 60°–80° occurs across FZA1855 where steep to overturned beds extend to the bottom hole.

A total of twelve fault zones identified in Hole A are located in the Plio-Pleistocene Cholan Formation, Pliocene Chinshui Shale, and Miocene Kueichulin Formation. Common fault rocks in the cores include intensely deformed fault core (clayey gouge) and adjacent highly fractured damage zones (fault breccia). The fault gouge is composed of ultra-fine-grained clay minerals and massive to foliated fabrics; occasionally, thin layers of indurate black material appear within the gouge zone. A typical example is the Chelungpu fault zone, FZA1111 (Fig. 2). The fault is bedding-parallel consisting of fault breccia and fault gouge 1109 m to 1112 m.

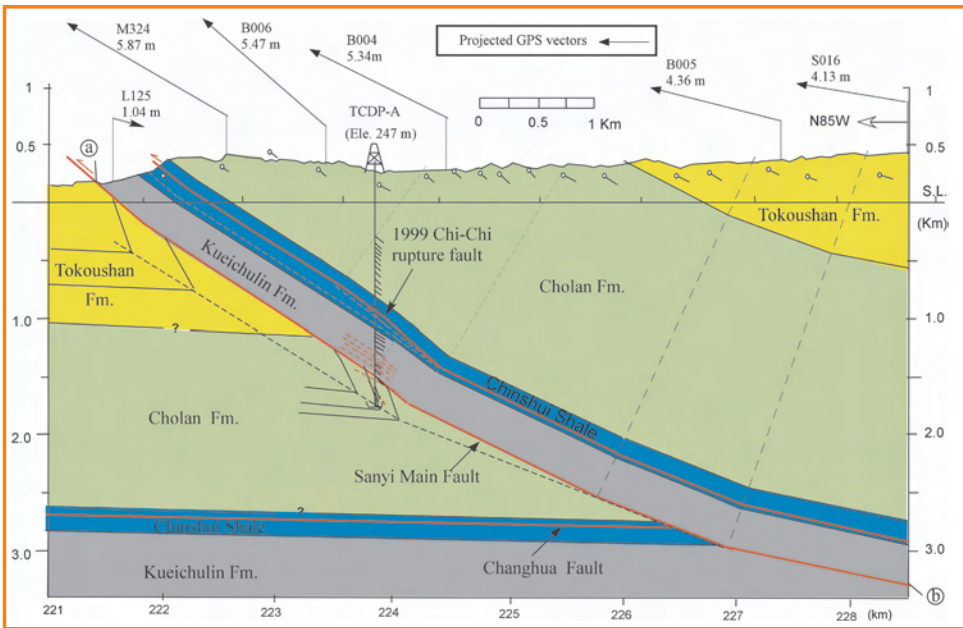

Figure 1. Interpreted structural profile across the Dakeng well (Hole A) based on the surface and subsurface drilled data. Measured depth (from rig floor, 3 m above the ground level) intervals and true thickness (in parenthesis) of formations in this borehole includes: Cholan, 0–1013 m (877 m); Chinshui, 1013–1300 m (249 m); and Kueichulin, 1300–1712 m (357 m). Underlying the Sanyi fault is the repeated section of Cholan formation from 1712–2003 m. Locations of Chelungpu (Chi-Chi rupture), Sanyi, and interpreted Changhua faults are shown by solid lines. Older faults formed prior to the Chi-Chi earthquake are shown by dashed lines. The displacement of the Sanyi fault is greater than 9 km (from eroded base of hanging-wall cutoff point "a" to footwall cutoff point "b"). The GPS vectors are projected components of the coseismic displacement in the plane of section (station number and displacement are given). Note that the displacement vectors, except in the footwall of the rupture fault, are approximately parallel to the fault at depth.

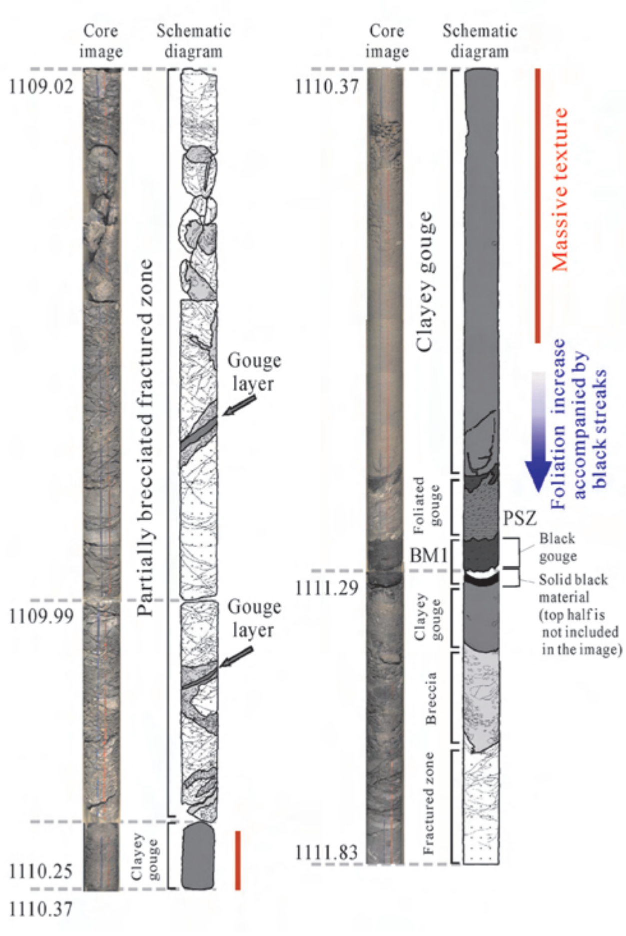

Figure 2. The core image and sketch diagram of fault zone FZA1111 from depth 1109.02 m to 1111.83 m of Hole A with descriptive comments. Note that the degree of deformation increases to the bottom of clayey gouge zone, and a 12-cm primary slip zone develops at depths of 1111.23–1111.35 m (from Ma et al., 2006).

The degree of fracturing increases from the top of the damage zone towards the gouge zone in which the fabrics changed from massive to foliate between 1110.25 m and 1111.35 m. The Chi-Chi major slip zone (MSZ, about 2 cm thick) is contained within the 12-cm-thick primary slip zone (PSZ), which is located near the bottom of this broad gouge zone (Ma et al., 2006).

In spite of large surface displacements, no temperature anomaly was observed near FZA1111 due to circulation of mud immediately after the drilling. Nevertheless, Kano et al. (2006) reported a heat anomaly of 0.06°C during repeated temperature measurements 6 months after the completion of drilling.

In situ Stress Measurements

Leak-off test: A standard commercial procedure of open-hole, extended leak-off tests was conducted in Hole B at depths between 940 m and 1350 m to determine *in situ* magnitudes of maximum (S_{Hmax}) and minimum (S_{Hmin}) horizontal stresses. Successful leak-off tests have been done at four locations in Hole B—1279.6, 1179.0, 1085.0, and

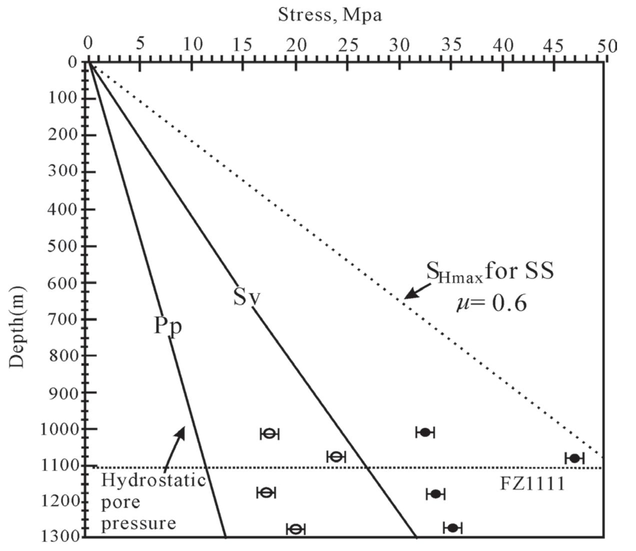

Figure 3. Plot of overburden stress (Sv) from integration of density logs, pore pressure, and S_{Hmax} (filled symbol) and S_{hmin} values (open symbol) determined from leak-off tests at different depths. The calculated upper bound S_{Hmax} (dashed line) for a strike-slip faulting stress regime assuming coefficient of friction μ=0.6 and location of FZA1111 are also shown.

1019.5 m—with two above and two below the FZB1137 (equivalent to FZA1111). Given the depth of overburden, we can calculate the vertical stress from integration of density logs and compile with pore pressure and hydrofracturing data from various depths (Fig. 3). The measurements clearly indicate a strike-slip fault regime after the Chi-Chi earthquake in this area.

Wellbore failure: *In situ* stresses S_{Hmax} determined from borehole breakouts and drilling-induced tensile fractures from Hole A and Hole B (Fig. 4) show that a significant change of S_{Hmax} azimuth occurs across the depth of 1300 m (also a stratigraphic boundary between the Chihsui shale and the Kueichulin Formation). The S_{Hmax} was oriented at 103°–138° with an average of 123° in the section of 700–1300 m, as opposed to 137°–164° (154° on average) from 1300 m to 1700 m. Borehole breakouts are relatively better developed in the Kueichulin Formation than in other places. This observation agrees with stronger anisotropy (stress magnitude) in the Kueichulin Formation, as shown by the shear wave anisotropy.

Shear Seismic Wave Anisotropy

Data from Dipole-Shear Sonic Imager (DSI™, Schlumberger) logs acquired over the interval of 508–1870 m in Hole A were used to assess shear wave velocity anisotropy. Analyses at these depths are shown by scatter plots and rose diagrams for nine discrete intervals of similar orientations of fast shear wave polarization (Fig. 5). A prominent NW-SE fast shear polarizing direction was generally observed except in a few depth zones, such as 738–770 m, 785–815 m, and 1517–1547 m. In particular, a very consistent mean direction with small dispersion of 115°±1°–2° (95% confidence interval) appears in the strongly anisotropic Kueichulin Formation at 1300–1650 m. Relatively consistent fast shear polarization directions appear across FZA1111 (average 165° between 1105 m and 1115 m) compared to the interval of 1078–1190 m with trending in a much broader range of 130°–170°. Thus, there is no observable systematic change of trend on fast shear polarization across the Chi-Chi slip zone. On the other hand, from the change of fast shear azimuth at depth 1000 m and contrasting dgree of anisotropy across the depth of 1300 m, the perturbation of regional stresses may have occurred within the upper and lower boundaries of the Chinshui Shale as suggested from detailed study of borehole breakouts (Wu et al., 2007).

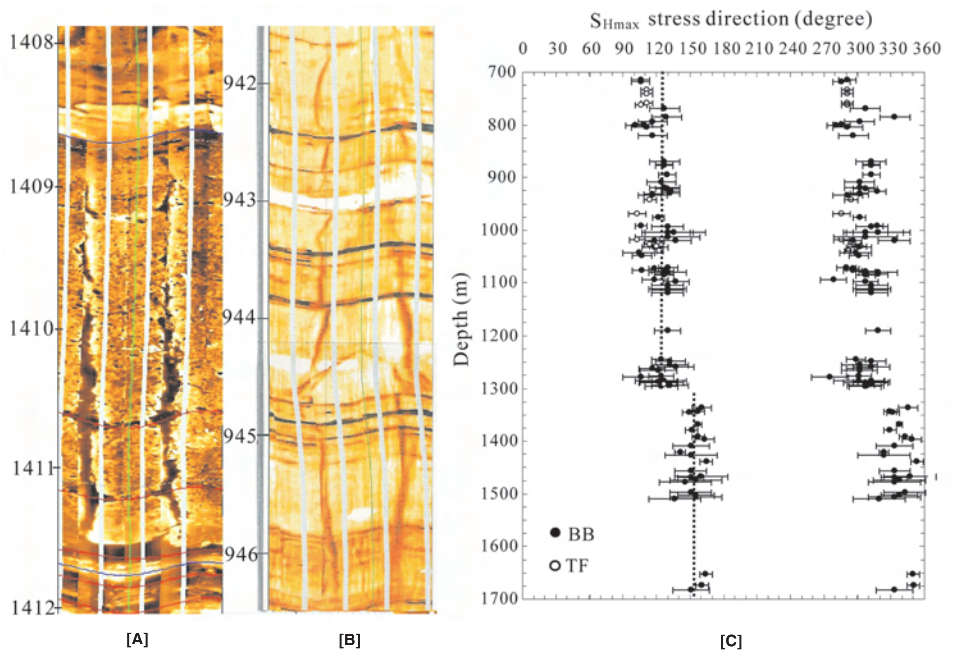

Figure 4. [A] Borehole breakouts as dark bands in opposite sides of the wellbore wall in FMI image logs of Hole A between 1409 m and 1411 m, and [B] drilling-induced tensile fractures in the Hole B at 941–947 m. [C] The plot of azimuth of S_{hmzx} determined from breakouts (BO) and tensile fractures (TF) in the TCDP wells. Width of bar shows an opening angle of BO and TF with dark and open circles, respectively, as mid-point. Dotted lines are average of mid-points between sections of 700–1300 m and 1300–1700 m.

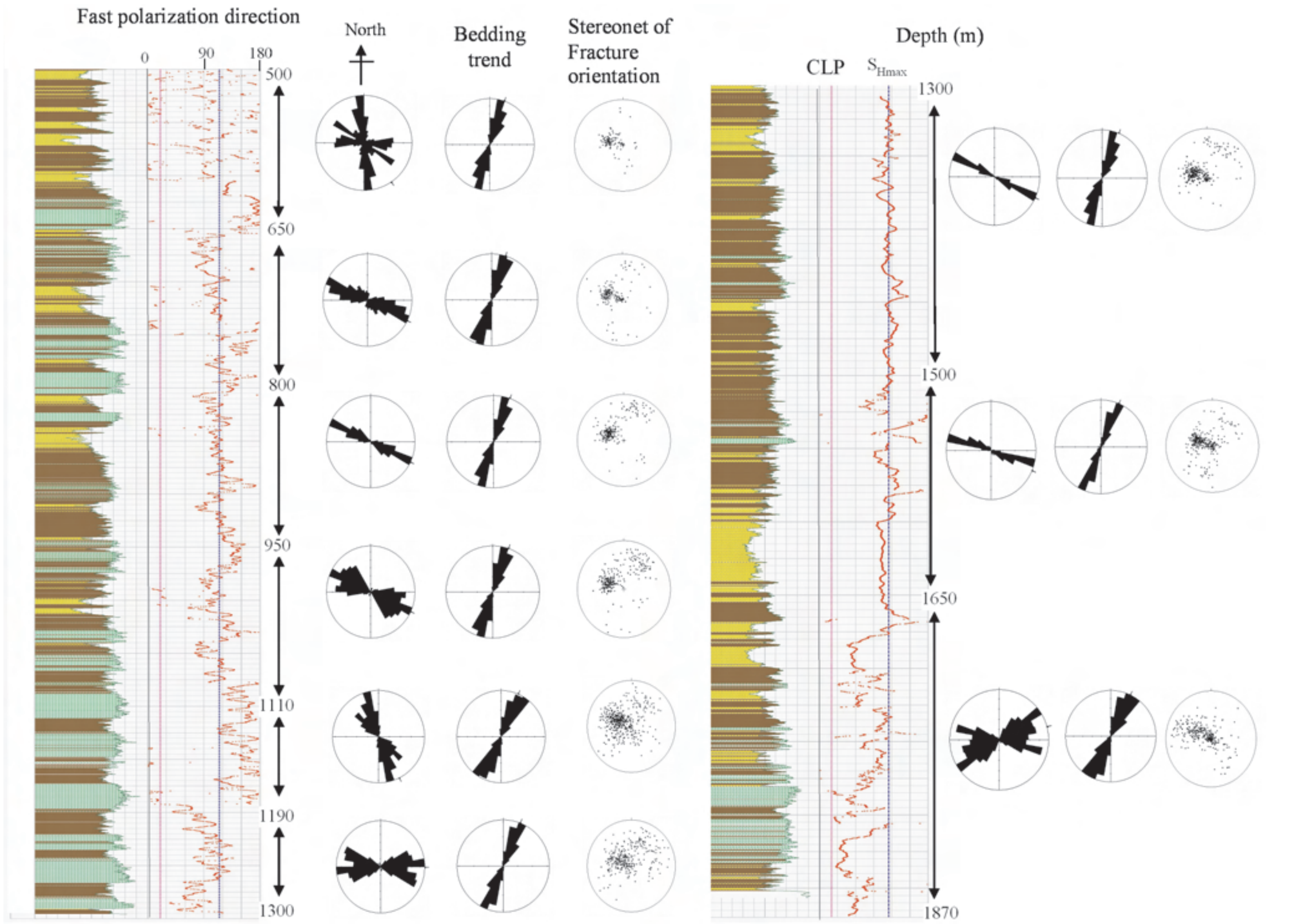

Figure 5. Comparison of the fast-shear polarization direction with bedding trend determined from borehole images and fracture orientations measured from core images. Azimuths of the Chelungpu fault (CLP, 020) and maximum horizontal stress (S_{hmax}, 115) in central Taiwan determined from earthquake focal mechanisms (Yeh et al., 1991) are shown for references.

Conclusions

The major scientific goal of the TCDP boreholes is to understand the physical mechanism involved in the large displacement during the Chi-Chi earthquake. We have attempted to answer this and relevant questions through studies of subsurface structure, fault-zone fabrics, formation physical properties and *in situ* stress state. Consistent correlations among fault zone fabrics, physical properties and clay mineralogy enable us to identify the bedding-parallel fault zone at depth 1111 m in Hole A being the rupture fault. FZA1111 is a 1-m gouge zone including 12 cm of thick indurate black material, and is characterized by: 1) bedding-parallel thrust fault with 30-degree dip; 2) the lowest resistivity; 3) low density, V_p and V_s; 4) high Vp/Vs ratio and Poisson's ratio; 5) low energy and velocity anisotropy, and low permeability within the homogeneous gouge zone; 6) increasing gas (CO_2 and CH_4) emissions, and 7) rich in smectite within the primary slip zone. The 2-cm wide, ultra fine-grained and foliated clay gouge near the bottom of the FZ1111 is interpreted to be the slip zone during the Chi-Chi earthquake. Ancillary investigation of temperature signal around the FZ1111 suggests that the slip zone is low frictional strength with both low coefficient of friction and low shear stress.

In situ stresses at the drill site were inferred from, leak-off tests, borehole breakouts and drilling-induced tensile fractures from borehole FMS/FMI logs, and shear seismic wave anisotropy from DSI logs. The dominant fast shear wave polarization direction is in good agreement with regional maximum horizontal stress axis, particularly within the strongly anisotropic Kueichulin Formation. A drastic change in orientation of fast shear polarization across the Sanyi thrust fault at the depth of 1712 m reflects the change of stratigraphy, physical properties and structural geometry.

Acknowledgements

The TCDP is primarily funded by Taiwan National Science Council (NSC), R.O.C. under the contract of NSC91-2119-M-008-030. We thank the International Continental Scientific Drilling Program (ICDP) for providing partial fund and technical consult. This research was supported by the Taiwan Earthquake Research Center (TEC) funded through NSC with grant number NSC94-2119-M-008-009. This article is a TEC contribution number 00021.

References

Kano, Y., Mori, J., Fujio, R., Ito, H., Yanagidani, T., Nakao, S., and Ma, K.-F., 2006. Heat signature on the Chelungpu fault associated with the 1999 Chi-Chi, Taiwan earthquake. *Geophys. Res. Lett.*, 33:L14306, doi:10.1029/2006GL026733.

Ma, K.-F., Tanaka, H., Song, S.-R., Wang, C.-Y., Hung, J.-H., Tsai, Y.-B., Mori, J., Yeh, E.-C., Soh, W., Sone, H., Kuo, L.-W., and Wu, H.-Y., 2006. Slip zone and energetics of a large earthquake from the Taiwan Chelungpu-fault Drilling Project. *Nature*, 444:473–476, doi:10.1038/nature05253.

Yeh, Y.-H., Barrier, E., Lin, C.-H., and Angelier, J., 1991. Stress tensor analysis in the Taiwan area from focal mechanisms of earthquake. *Tectonophysics*, 200:267–280, doi:10.1016/0040-1951(91)90019-O.

Yue, L.-F., Suppe, J., and Hung, J.-H., 2005. Structural geology of a classic thrust belt earthquake: the 1999 Chi-Chi earthquake Taiwan (Mw=7.6). *J. Struct. Geol.*, 27:2058–2083.

Wu, H.-Y., Ma, K.-F., Zoback, M., Boness, N.., Ito, H., Hung, J.-H., 2007. Stress orientations of Taiwan Chelungpu-Fault Drilling Project (TCDP) hole-A as observed from geophysical logs. *Geophys. Res. Lett.*, 34, L01303.

Authors

Jih-Hao Hung, Department of Earth Sciences and Institute of Geophysics, National Central University, No. 300, Jhongda Road, Johngli City, Taoyuan County, 32001, Taiwan (R.O.C.), e-mail:jhung@earth.ncu.edu.tw.

Kuo-Fong Ma, and Chien-Yin Wang, Department of Earth Sciences and Institute of Geophysics, National Central University, No. 300, Jhongda Road, Johngli City, Taoyuan County, 32001, Taiwan (R.O.C.).

Sheng-Rong Song, Department of Geosciences, National Taiwan University, No. 1, Sec. 4, Roosevelt Road, Taipei, 10617, Taiwan (R.O.C.).

Hisao Ito, Center for Deep Earth Exploration (CDEX), Japan Agency for Marine-Earth Science and Technology (JAMSTEC), 3173-25 Showa-machi, Kanazawa-ku, Yokohama, Kanagawa 236-0001, Japan.

Weiren Lin and En-Chao Yeh, Kochi Institute for Core Sample Research, Japan Agency for Marine-Earth Science and Technology (JAMSTEC), B200 Monobe, Nankoku, Kochi, 783-8502, Japan.